SIMULATION ANALYSIS OF A TARGET ANGLE ESTIMATOR

(2)

D. J. KERSHAW

Simulation Analysis of a Target Angle Estimator

D.J. Kershaw

MRL Technical Note
MRL-TN-626

Abstract

Most underwater tracking applications require the estimation of target angle, whether in azimuth or elevation. In this note, the effect of integration time on the performance of a simple target angle estimator has been analysed via computer simulation. The simulated estimator mean is shown to match theoretical calculations of the mean of the estimator for time-bandwidth products from 5 to 100. Computed variance results are also presented. Some practical considerations for the simulation of narrow bandwidth processes are discussed.

DSTO MATERIALS RESEARCH LABORATORY

Contents

Simulation Analysis of a Target Angle Estimator

1. Introduction

The area of torpedo countermeasures, for surface ship and submarine defence, is a current activity at MRL. A necessary part of this study is the understanding of the effect of different signal processing structures on torpedo performance. In this technical note a processing structure that could be implemented using analog techniques is analysed using computer simulation. Only target angle estimation is considered.

In order to home onto targets the torpedoes must estimate the target azimuth and elevation angles, relative to the torpedo heading. The conventional technique is to estimate the time delay, or phase shift, between signals received from two spatially separated receivers. These signals would usually be the left and right beam inputs formed by summing different sets of elements in a transducer array (if considering azimuth angle estimation). When in active mode the signals of interest are often in a narrow band around the transmitted frequency, allowing narrow band signal theory to be used. As most torpedoes use the same input processing for both active and passive mode operation the narrow band assumption is also valid for passive mode and is the approach taken in this note.

2. Estimator Structure

For convenience consider the problem of a target manoeuvring in a horizontal plane. The geometry of the problem is illustrated in Figure 1. Target physical angle ϕ is measured relative to the centre of the array, while left and right indicate the effective spatial location of the left and right beam signals formed by summing different elements in the transducer array. The target signal and the background noise are assumed to be independent white Gaussian noise processes. The electrical phase

difference between the left and right signals is θ, and is related to the target physical angle ϕ by the transducer beam patterns.

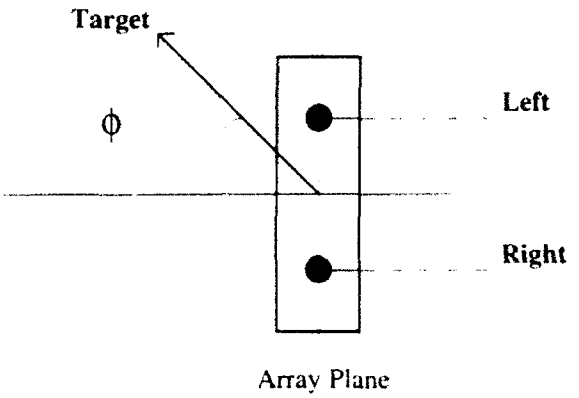

Figure 1: Transducer array geometry

A typical input processing scheme is shown in Figure 2. The signals are filtered by bandpass filters, usually centred at the receiving frequency for a stationary target (assuming an active sonar), with the bandwidth covering the expected range of Doppler shifts. For example, a system with a transmission frequency of 25 kHz would require a 2 kHz bandwidth to detect targets with speeds of up to ± 58 knots, hence the noise processes forming the left and right input signals, after the bandpass filters, can be considered to be narrow band processes. The scheme as shown would be suitable for passive systems, active systems could use the scheme in conjunction with appropriate signal detection processing to indicate whether a valid return is present.

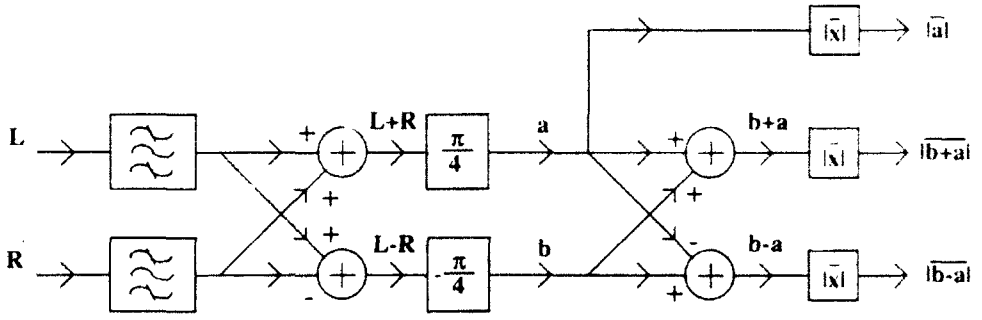

Figure 2: Input processing scheme

The sum and difference signals are formed to aid the recovery of the phase shift between the left and right signals. As shown in Figure 2, further phase shifting and combining of the sum and difference signals is performed before the signals are magnitude detected and integrated with a smoothing time constant T. The minimum

integration time is the inverse of the bandpass filter bandwidth B (Hz), giving a minimum time-bandwidth product (BT) of unity. An estimator is proposed which uses the integrated signals to recover the electrical phase angle via the transformation

$$\xi = 2\arctan(c) \tag{1}$$

where

$$c = \frac{\mathrm{E}(|b+a|) - \mathrm{E}(|b-a|)}{2\mathrm{E}(|a|)}. \tag{2}$$

In the above equation ξ is the estimator for the electrical phase angle θ and $\mathrm{E}(x)$ stands for the expected value of x. If the estimator is unbiased then the expected value (mean) of the estimator, ξ, will be θ.

3. *Analytic Description*

3.1 Analytic Signals

For the system in Figure 2, with white Gaussian noise input processes (passive operation), the left and right signals after the bandpass filters can be written as

$$L = N_{11}\cos\omega_0 t + N_{12}\sin\omega_0 t + S_{11}\cos(\omega_0 t + \theta/2) + S_{12}\sin(\omega_0 t + \theta/2) \tag{3a}$$

and

$$R = N_{21}\cos\omega_0 t + N_{22}\sin\omega_0 t + S_{11}\cos(\omega_0 t - \theta/2) + S_{12}\sin(\omega_0 t - \theta/2) \tag{3b}$$

where N_{11}, N_{12}, N_{21} and N_{22} are independent Gaussian noise sources, representing the background noise, each with zero mean and variance σ_N^2. Similarly, S_{11} and S_{12} are also independent white Gaussian noise sources, representing the target source signal, with zero mean and variance σ_S^2 while ω_0 is the centre frequency of the bandpass filters.

As written in eqn. (3), the input equations contain both envelope and carrier components. The carrier can be removed from the equations as the information content of the signal is only in the envelope of the signal. To do this the complex, or analytic, signal representation is used. If $x(t)$ is a real narrow band signal, its analytic equivalent is denoted $\tilde{x}(t)$ and is related to the real signal by [1]

$$\tilde{x}(t) = 2\left(x(t)e^{-j\omega_0 t}\right)_{\mathrm{LPF}} \tag{4a}$$

and

$$x(t) = \mathrm{Re}\left[\tilde{x}(t)e^{j\omega_0 t}\right], \tag{4b}$$

where LPF stands for Low Pass Filter, and $j = \sqrt{-1}$.

Using this notation, the input signal equations can be rewritten as

$$\tilde{L} = \tilde{S}e^{j\theta/2} + \tilde{N}_1 \tag{5a}$$

and

$$\tilde{R} = \tilde{S}e^{-j\theta/2} + \tilde{N}_2 \ , \tag{5b}$$

where $\tilde{S} = S_{11} - jS_{12}$, $\tilde{N}_1 = N_{11} - jN_{12}$, and $\tilde{N}_2 = N_{21} - jN_{22}$.

In the next section this formulation is used to develop the estimator equations in terms of the input noise processes.

3.2 *Estimator Equations*

The processing structure of Figure 2 is still valid for the analytic signal representation, noting that all processing is now using complex signals rather than real signals. The signals after phase shifting, $(\tilde{a}, \tilde{b})$, can be written in terms of the $\tilde{L}$ and $\tilde{R}$ signals to form

$$\tilde{a} = \left(\tilde{L} + \tilde{R}\right)e^{j\pi/4} \tag{6a}$$

and

$$\tilde{b} = \left(\tilde{L} - \tilde{R}\right)e^{-j\pi/4} \ . \tag{6b}$$

Using the expressions in eqn. (6), substituting for $\tilde{L}$ and $\tilde{R}$ from (5), and with some manipulation, expressions for the input signals to the magnitude detection and averaging blocks in the processing structure can be obtained. These are

$$\tilde{a} = \left(2\tilde{S}\cos\frac{\theta}{2} + \tilde{N}_1 + \tilde{N}_2\right)e^{j\pi/4} \tag{7}$$

$$\tilde{b} + \tilde{a} = \sqrt{2}\left\{\tilde{S}\left(\cos\frac{\theta}{2} + \sin\frac{\theta}{2}\right)(1+j) + \tilde{N}_1 + j\tilde{N}_2\right\} \tag{8}$$

and

$$\tilde{b} - \tilde{a} = -\sqrt{2}\left\{\tilde{S}\left(\cos\frac{\theta}{2} - \sin\frac{\theta}{2}\right)(1+j) + \tilde{N}_2 + j\tilde{N}_1\right\} \ . \tag{9}$$

Before these expressions can be used in the final estimator equation (eqn. (2)) the magnitude of the complex number must be taken and then averaged over several consecutive magnitude values. In general this calculation would require the probability distributions of the above quantities, and is a multivariate problem when

more than a single magnitude measurement is considered. However, an asymptotic expression for the expected value of the estimator mean can be calculated. The estimator mean will approach the asymptotic result for either long integration (averaging) length or large signal-to-noise ratios. Let $\tilde{x} = x_1 - jx_2$, where x_1 and x_2 are independent zero mean white Gaussian noise processes with equal variance σ_N^2 then [2, p.195]

$$E(|\tilde{x}|) = E\left(\sqrt{x_1^2 + x_2^2}\right) = \sqrt{\frac{\pi}{2}}\sigma_x = \frac{\sqrt{\pi}}{2}\sqrt{E\left(\tilde{x}.\tilde{x}^*\right)} . \qquad (10)$$

The expected values can now be calculated using eqn. (10) remembering that $\tilde{S}$, $\tilde{N}_1$, and $\tilde{N}_2$ are independent complex white Gaussian noise processes with twice the variance of their components. After some calculation the expected value for c (eqn. (2)) can be shown to be

$$E(c) = \frac{\sqrt{8\sigma_\xi^2\left(\cos\frac{\theta}{2} + \sin\frac{\theta}{2}\right)^2 + 8\sigma_\xi^2} - \sqrt{8\sigma_\xi^2\left(\cos\frac{\theta}{2} - \sin\frac{\theta}{2}\right)^2 + 8\sigma_\xi^2}}{2\sqrt{8\sigma_\xi^2\cos^2\frac{\theta}{2} + 4\sigma_\xi^2}} \qquad (11)$$

As a result of the additive noise, eqn. (11) will be a biased estimate of θ for all input cases except the infinite signal-to-noise ratio. In this case eqn. (11) can be shown to reduce to

$$E(c) = \tan\frac{\theta}{2} . \qquad (12)$$

Substituting this in eqn. (1) yields

$$E(\xi) = \theta , \qquad (13)$$

which is the expected result for the estimator. Letting $S = 2\sigma_N^2$ and $N = 4\sigma_N^2$, eqn. (11) and eqn. (1) can be combined to specify the asymptotic performance of the proposed estimator for any signal-to-noise ratio. Denoting the asymptotic result by $\bar{\xi}$ the result is

$$\bar{\xi} = 2\arctan\left\{\frac{\sqrt{1+\frac{2S}{N}\left(\cos\frac{\theta}{2}+\sin\frac{\theta}{2}\right)^2} - \sqrt{1+\frac{2S}{N}\left(\cos\frac{\theta}{2}-\sin\frac{\theta}{2}\right)^2}}{\sqrt{2}\sqrt{1+\frac{4S}{N}\cos^2\frac{\theta}{2}}}\right\} . \qquad (14)$$

4. *Simulation Model*

The estimator, as defined in section 2, was simulated using the Signal Processing Workstation software package, running on a Sun Sparcstation SLC hardware platform. The Signal Processing Workstation, or SPW, is a graphical based simulation tool which allows the user to quickly develop simulation models for signal processing systems. Models are developed using basic building blocks, with the input processing shown schematically in Figure 2 translating directly into the basic building blocks. The model is completed with the addition of signal source and sink blocks, allowing specification of input signals and viewing of output signals.

Analytic signal representation allows significant computational savings in the simulation model. For a system operating at 25 kHz, with a 2 kHz bandwidth, the minimum sampling rate, using real signals without bandpass sampling, would be 52 kHz. As the processing scheme being considered has phase shifts between the input signals, the sampling rate would have to be high enough to allow the phase shifts to be implemented as a time delay between the signal components of the input signals. If 20 samples/cycle at 25 kHz are desired then a sampling rate of 500 kHz is required. The $\pm \pi/4$ phase shifts in the scheme also present difficulties if real signals are used. Another concern is the need to implement narrow band white noise sources for the input signals. While this is straightforward, the calculations add significantly to the computational load and complexity of the final model

Basing the model on analytic signals overcomes many of these concerns. The major advantage is that the required sampling rate is dictated by the envelope bandwidth and not by the carrier frequency. As the signals are now complex the sampling rate can be set equal to the bandwidth, while phase shifts are implemented by a multiplication of the signal by $e^{j\alpha}$ where α is the phase shift. For the scheme considered in this note, one result is that all references to frequency are removed from the model with each sample representing a time-bandwidth product (BT) of unity. The required noise sources are now simply white noise sources with no further processing required. The computational effort for the analytic model is approximately three orders of magnitude less than for the real simulation model.

5. *Results*

Monte Carlo simulations were performed for time-bandwidth products of 5, 10, 25, 50 and 100. For each case 100 passes were used to evaluate the mean and variance of the estimator. Figures 3, 4 and 5 show the estimator mean results for BT = 100, 25 and 5, with the asymptotic results calculated using eqn. (14) included for comparison.

The signal-to-noise ratios shown are $10 \log_{10} S/N$. The BT = 100, and BT = 25 are very close to the asymptotic results, while the estimator mean for BT = 5 is starting to deviate from the asymptotic results, the degradation being due to the short integration time.

The effect of varying the integration time on estimator performance is more clearly shown in the variance results. In figures 6, 7 and 8 the estimator variance, $E((\xi - \bar{\xi})^2)$ has been plotted against different time-bandwidth products for fixed signal-to-noise ratio. The degradation in estimator performance is shown by the rapid increase in estimator variance as the integration time is decreased.

Figures 9, 10 and 11 show the output ξ from Monte Carlo runs for BT = 100, 25 and 5, with 0 dB signal-to-noise ratio. These show the estimated angles, as a function of time (sample number), for a hypothetical target that has an initial target electrical angle of 0° and increases in 20° steps after every 100 samples for a total of 1000 samples. The final target electrical angle is 180°. As expected the Monte Carlo results for BT = 100 are localised around the expected values, while the variation in the expected values increases as the BT product decreases.

The variance results presented in this note are for the analytic system. If the processing were to be implemented as a real signal system then these results could only be used as an indication of the variation in the real signal variances as the integration time and signal-to-noise ratios are varied. Quantitative values for the real signal variance results could be obtained via a full real signal simulation, with associated computational expense. Alternatively the system can be analysed using a probabilistic approach [2] to determine the relationship between the real and analytic signal variance results.

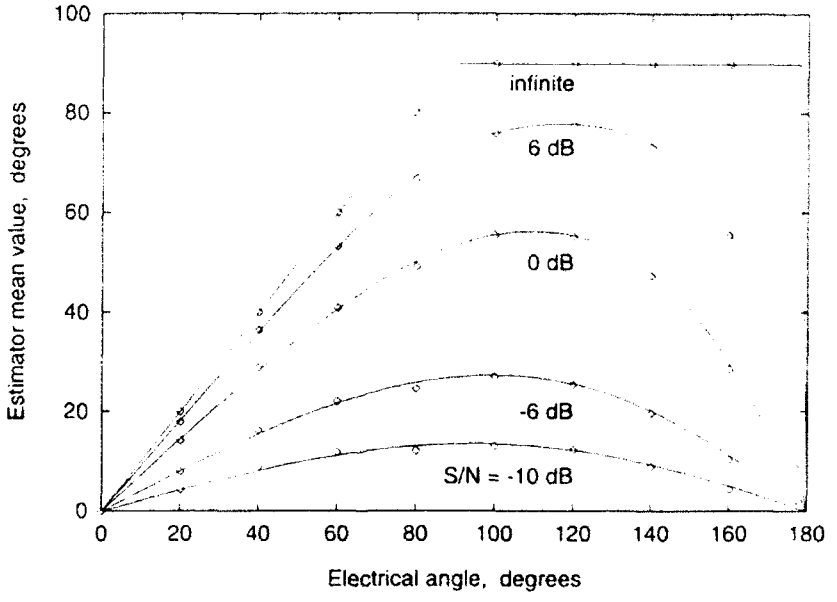

Figure 3: *Estimator mean for BT = 100 (lines - asymptotic values, points - simulation values).*

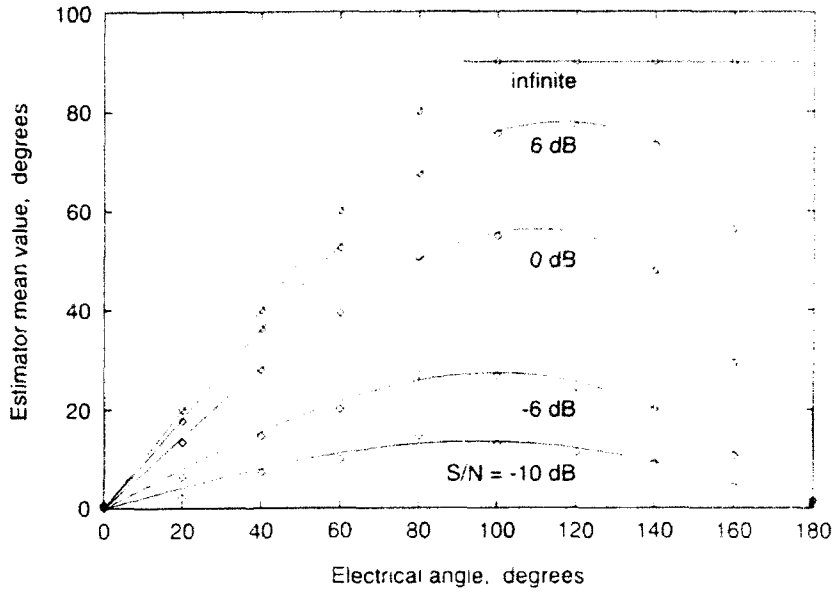

Figure 4: *Estimator mean for BT = 25 (lines - asymptotic values, points - simulation values).*

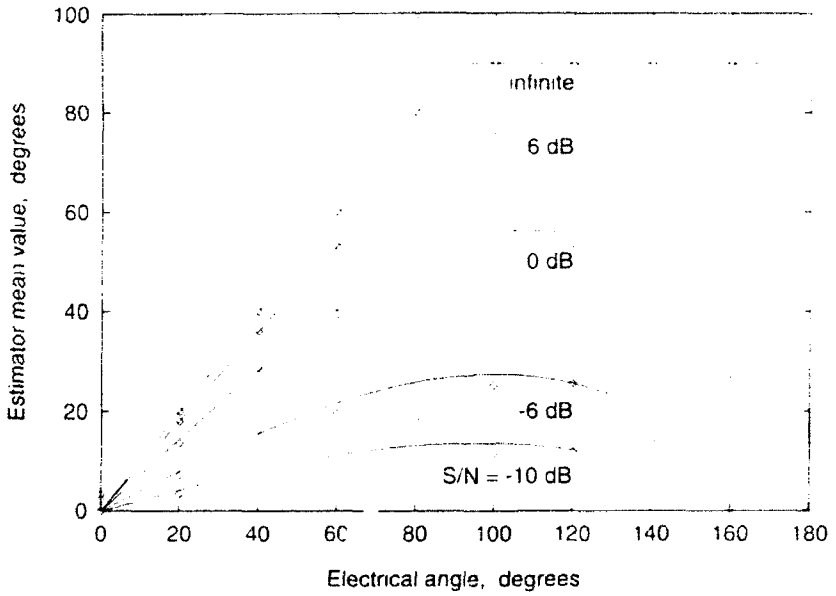

Figure 5: *Estimator mean for BT = 5 (lines - asymptotic values, points - simulation values).*

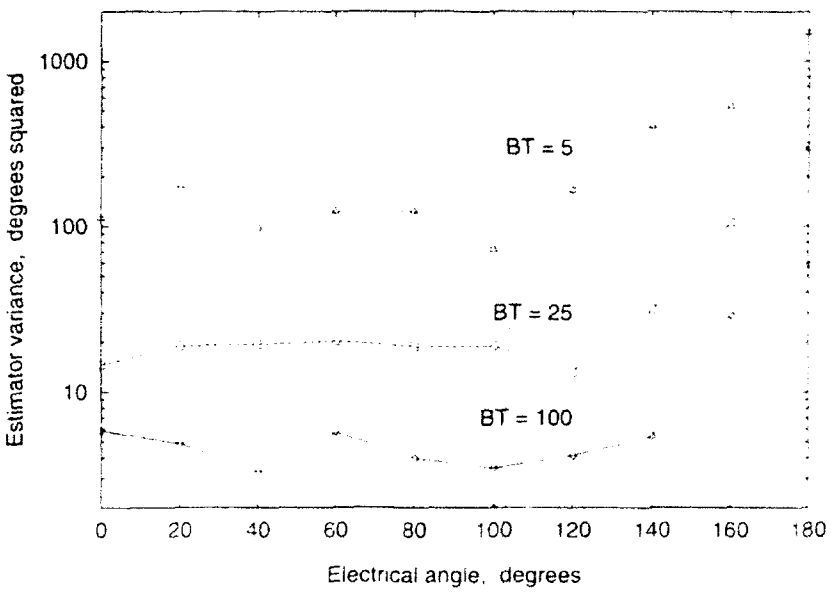

Figure 6: Estimator variance, signal-to-noise ratio = 6 dB.

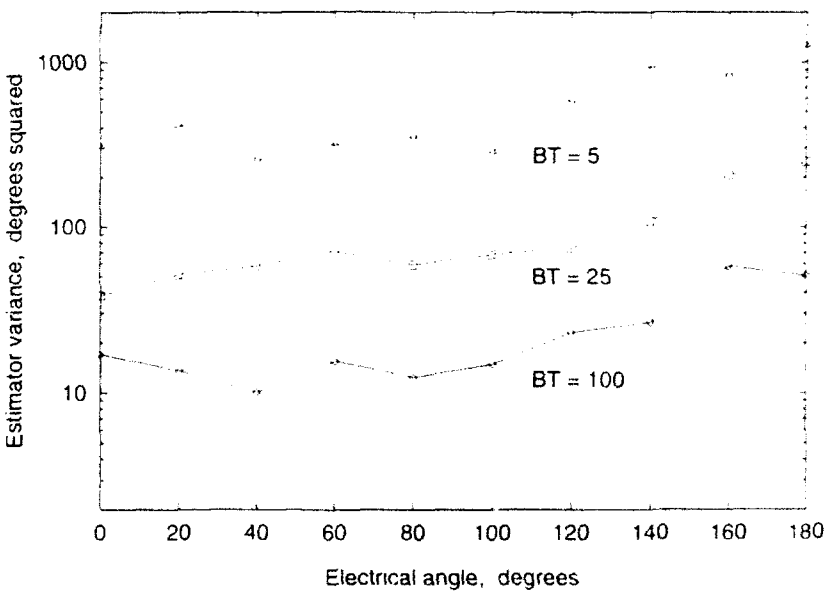

Figure 7: Estimator variance, signal-to-noise ratio = 0 dB.

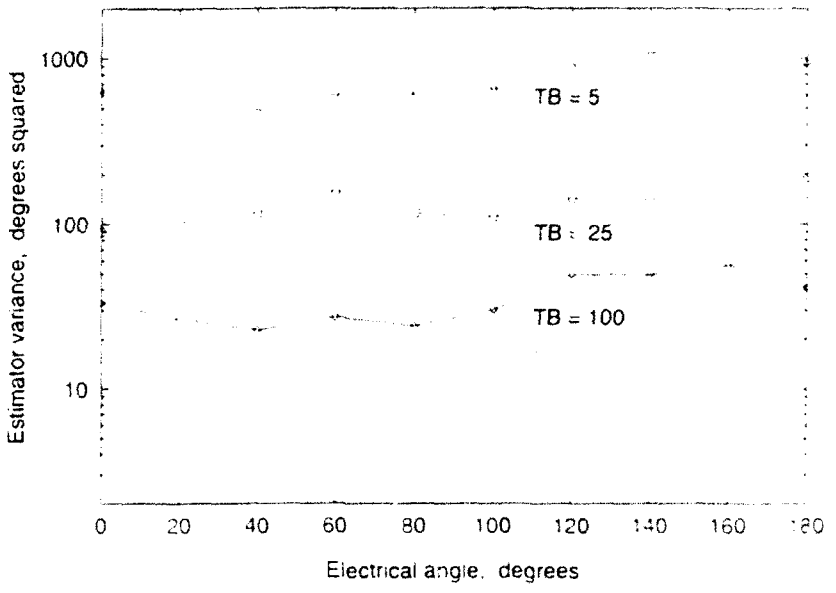

Figure 8: Estimator variance, signal-to-noise ratio = - 6 dB.

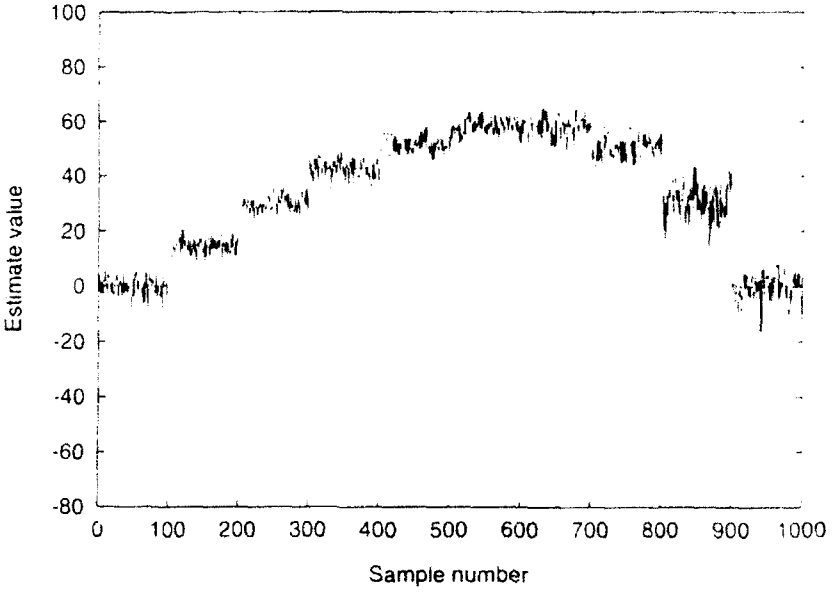

Figure 9: Monte Carlo raw output, BT = 100 (signal-to-noise = 0 dB).

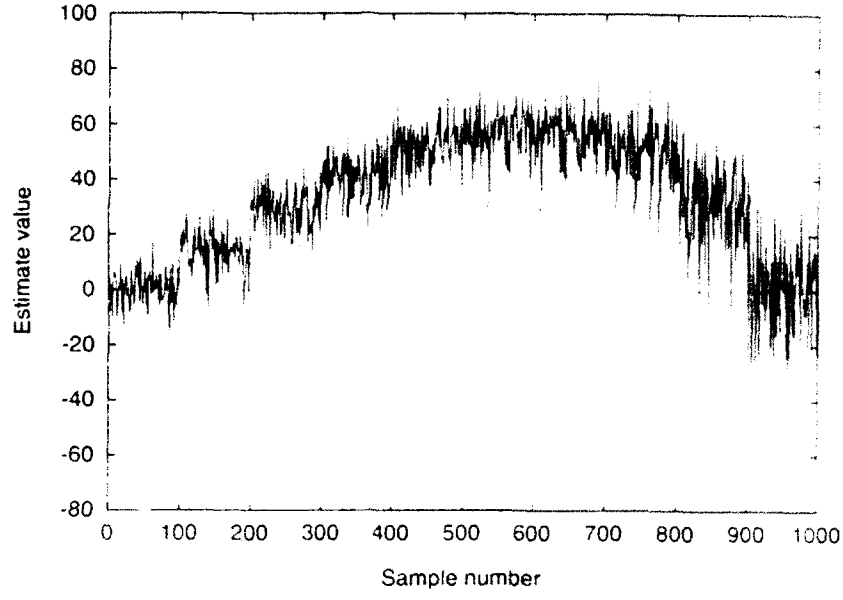

Figure 10: *Monte Carlo raw output, BT = 25 (signal-to-noise = 0 dB).*

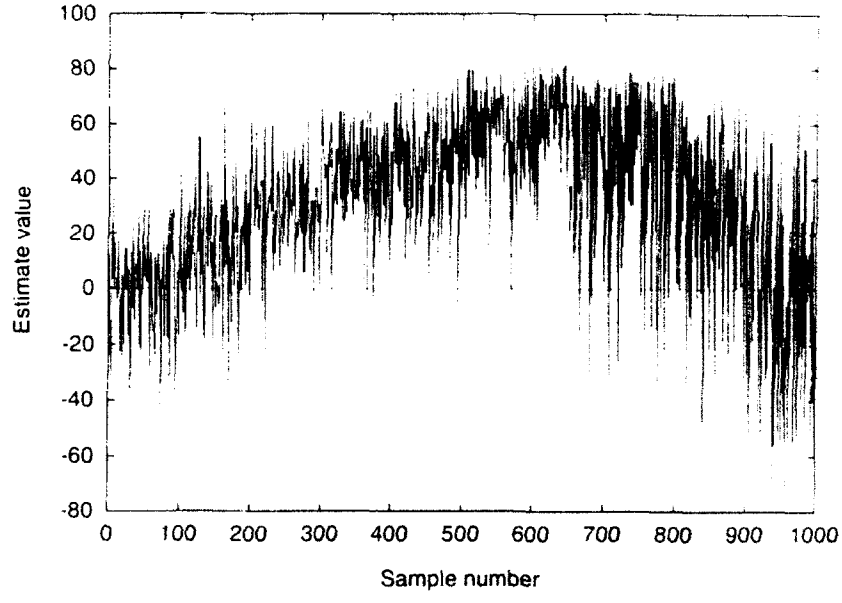

Figure 11: *Monte carlo raw output, BT = 5 (signal-to-noise = 0 dB).*

6. Conclusion

The effect of integration time on the performance of a target angle estimator has been analysed via computer simulation. An asymptotic expression was developed for the estimator mean and compared to the simulation results. The results obtained for the mean are valid for both real and analytic models of the estimator processing structure, while the variance results can only be used as a qualitative measure of the variance for the real simulation model.

7. References

1. Van Trees, H.L. (1971). *Detection estimation and modulation theory*, Volume 3 New York: Wiley.

2. Davenport, W.B. and Root, W.B. (1958). *Random signals and noise*, McGraw-Hill.

SECURITY CLASSIFICATION OF THIS PAGE **UNCLASSIFIED**

REPORT NO.	AR NO.	REPORT SECURITY CLASSIFICATION
MRL-TN-626	AR-008-230	Unclassified

TITLE

Simulation analysis of a target angle estimator

AUTHOR(S)
D.J. Kershaw

CORPORATE AUTHOR
DSTO Materials Research Laboratory
PO Box 50
Ascot Vale Victoria 3032

REPORT DATE	TASK NO.	SPONSOR
January, 1993	NAV 89/020	RAN

FILE NO.	REFERENCES	PAGES
G6/4/8-4340	2	17

CLASSIFICATION/LIMITATION REVIEW DATE

CLASSIFICATION/RELEASE AUTHORITY
Chief, Maritime Operations Division

SECONDARY DISTRIBUTION

Approved for public release

ANNOUNCEMENT

Announcement of this report is unlimited

KEYWORDS

Monte Carlo simulations
Signal to noise ratios
TBA
Target angle estimation

ABSTRACT

Most underwater tracking applications require the estimation of target angle, whether in azimuth or elevation. In this note, the effect of integration time on the performance of a simple target angle estimator has been analysed via computer simulation. The simulated estimator mean is shown to match theoretical calculations of the mean of the estimator for time-bandwidth products from 5 to 100. Computed variance results are also presented. Some practical considerations for the simulation of narrow bandwidth processes are discussed.

Simulation Analysis of a Target Angle Estimator

D.J. Kershaw

(MRL-TN-626)

DISTRIBUTION LIST

Director, MRL
Chief, Maritime Operations Division
Dr C.I. Sach
D.J. Kershaw
Task Sponsor (Director, Submarine Policy & Warfare, Russell Offices A-G-11, Canberra
Attention: CMDR J. Taubman and LCDR R. Drain) (2 copies)
MRL Information Service

Chief Defence Scientist (for CDS, FASSP, ASSCM) (1 copy only)
Director, Surveillance Research Laboratory
Director (for Library), Aeronautical Research Laboratory
Director, Electronics Research Laboratory
Head, Information Centre, Defence Intelligence Organisation
OIC Technical Reports Centre, Defence Central Library
Officer in Charge, Document Exchange Centre (8 copies)
Army Scientific Adviser, Russell Offices
Air Force Scientific Adviser, Russell Offices
Navy Scientific Adviser, Russell Offices - data sheet only
Scientific Adviser, Defence Central
Director-General Force Development (Land)
Senior Librarian, Main Library DSTOS
Librarian, MRL Sydney
Librarian, H Block
UK/USA/CAN ABCA Armies Standardisation Rep c/- DGAT (8 copies)
Librarian, Australian Defence Force Academy
Counsellor, Defence Science, Embassy of Australia - data sheet only
Counsellor, Defence Science, Australian High Commission - data sheet only
Scientific Adviser to DSTC, C/- Defence Adviser - data sheet only
Scientific Adviser to MRDC, C/- Defence Attache - data sheet only
Head of Staff, British Defence Research and Supply Staff (Australia)
NASA Senior Scientific Representative in Australia
INSPEC: Acquisitions Section Institution of Electrical Engineers
Head Librarian, Australian Nuclear Science and Technology Organisation
Senior Librarian, Hargrave Library, Monash University
Library - Exchange Desk, National Institute of Standards and Technology, US
Exchange Section, British Library Document Supply Centre
Periodicals Recording Section, Science Reference and Information Service, UK
Library, Chemical Abstracts Reference Service
Engineering Societies Library, US
Documents Librarian, The Center for Research Libraries, US